ACS OMEGA

Open Access

http://pubs.acs.org/journal/acsodf

Article

Distribution of Carbon Nanotubes in an Aluminum Matrix by a Solution-Mixing Process

Navin Kumar, Shatrughan Soren,* Akhileshwar Nirala, Naif Almakayeel, T. M. Yunus Khan, and Mohammad Amir Khan

Cite This: *ACS Omega* 2023, 8, 33845−33856

Read Online

ACCESS | Metrics & More | Article Recommendations

ABSTRACT: In order to overcome the limitations of standard ball-mill mixing processes to fabricate a uniformly dispersed carbon nanotube (CNT) reinforcement composite without damaging CNTs in matrix powder, a unique and easy solution-mixing process was developed. The present study aims to synthesize Al-0.5 wt % CNT composites using ball-milling and solution-mixing processes and compares their CNT dispersion and structural and thermal properties. Compared with the ball-milling process, the solution-mixing process was simple and effective for the uniform distribution of CNTs without structural damage. Various methods were utilized to examine the structural characteristics of the composite powder. These techniques included high-resolution transmission electron microscopy (HRTEM), X-ray diffraction (XRD), field emission scanning electron microscopy (FESEM), Raman spectroscopy, and particle size analysis. Raman spectroscopy observes an increase of defects in ball-milled composites, and the particle size analyzer confirms the structural deformation, resulting in the degradation of composite powder mechanical properties. In the solution-mixing process, aluminum particles and the structure of CNTs are well-preserved even after mixing. Thermogravimetric analysis (TGA) was used to research the thermal stability of the composite materials. The results validated the impact of CNTs on thermal characteristics enhancement (improved thermal resistance) when compared with pure aluminum, suggesting potential uses in the aerospace industry, transport, and construction sectors.

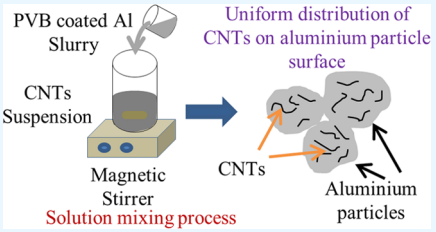

1. INTRODUCTION

In recent decades, carbon nanotubes (CNTs) have become extremely popular as materials of choice for manufacturing lightweight composites of metal matrix, which are known as metal matrix composites (MMCs). The exceptional properties of CNTs have drawn the attention of researchers in particular. High melting point and remarkable electrical and thermal conductivity, as well as chemical stability, are a few of them, even when exposed to high temperatures. The experimental observation on CNT has revealed low density (∼1.2−1.8 g/cm^3), large surface area (∼1000 m^2/g) with high aspect ratios (∼50−500), elastic modulus (1 TPA), hydrogen storage potential,[1−3] corrosion resistance,[4] solid lubricant,[5,6] and remarkable optical and biological properties.[7,8] These properties make CNTs a suitable reinforcement material for metal matrix and ceramic matrix composites.[9,10] The most commonly used reinforcement materials are SiC,[11,12] Al_2O_3,[13] ZnO,[14] Ti,[15] graphite,[16] graphene,[17] CNTs,[18−20] and others for the fabrication of Al metal matrix composites. CNT/Al composites have emerged as potential structural materials for lightweight applications requiring high strength and anticorrosion in the automotive and aerospace sectors. The automobile and aerospace sectors currently focus on developing the latest aircraft and vehicles able to perform at higher speeds and temperatures and run long distances before maintenance with structural weight reduction. The low weight of CNTs/Al composites improves fuel economy and lowers pollutants that harm the environment and the climate and cause human deaths. Al/CNT composites are also recognized as the most sought-after materials for a wide range of applications, including nanoelectronics, the medical sector, energy storage devices, nanosensors, smart materials, and biological sciences.[21,22]

CNTs as a reinforcement material are not explored up to the mark due to the difficulty in their uniform distribution with the matrix material because of the affinity of CNT accumulation due to van der Waals forces.[23−25] The presence of agglomerates will result in a lesser density and more voids in the bulk materials. As a result of CNT agglomerates restricting diffusion between aluminum particles, there would be larger gaps in the overall composite, which would reduce the density, ultimately deteriorating the overall characteristics. CNTs must be consistently dispersed in the Al matrix to realize the

Received: June 25, 2023
Accepted: August 16, 2023
Published: September 3, 2023

https://doi.org/10.1021/acsomega.3c04531
ACS Omega 2023, 8, 33845−33856

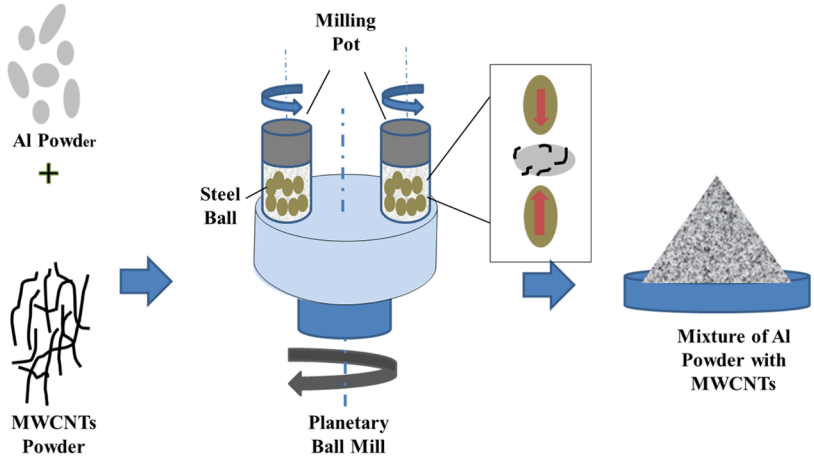

Figure 1. Ball-milling process schematic representation.

maximum potential of reinforcements. Mechanical mixing, in situ synthesis, and molecule-level mixing have all been used to distribute carbon nanotubes into metal matrices. Only Cu, Co, and Ni matrix composites reinforced with CNTs can be made utilizing molecular-level mixing. Growing CNTs in situ indicated catalyst particle impurity issues and was incompatible with methods used to fabricate industrial composites. Mechanical dispersion techniques (such as ball-milling) have an issue of CNT structural degradation.

Experts consider Al-CNT composites as potential materials for aerospace and automobile industries because of their excellent properties.[26,27] The preceding literature has a large number of research publications on the synthesis and characterization of Al/CNT nanocomposite materials and structures.[28−32] Liu et al.[33] investigated adsorbing the dispersed CNTs on the Al surface. The aqueous CNT zwitterionic surfactant solution was mixed with flaky Al powders made by ball-milling the Al particles. After filtering and drying, CNTs were adsorbed onto flaky Al particles to create CNT/Al powders with a maximum CNT concentration of 7.5 vol %. To make composites with 1.5 and 3 vol % CNT/Al, powder metallurgy was used with the composite powders. Choi et al.[31] want to disperse CNTs in Al powder in their experiment. They used a mixing jar with CNTs (4.5 vol %) and aluminum powder (99.5% purity, 50 μm in average diameter), as well as stainless steel balls (5 mm in diameter), as the milling medium, to disperse CNTs in the aluminum powder. The powder combination was then stirred in a pure argon atmosphere at room temperature with horizontal impellers rotating at a predetermined speed (the ball-to-powder weight ratio was 15:1). To prevent the powder from clogging together, 1 wt % stearic acid ($CH_3(CH_2)_{16}COOH$) was added as a control agent. In a 250 mL stainless steel container, 100 g AA5083 powder was blended with varying amounts (0−2.0 wt %) of CNT by Stein et al. They milled the composite powder in a planetary mill using stainless steel milling balls having a diameter of 10 mm and a ball-to-powder weight ratio of 2:1, for 240 min at 600 rpm (rpm). CNTs uniformly dispersed, but the structure of CNTs was damaged.

Based on the above-referred research, the significant challenges in developing Al metal composites with CNTs as reinforcement are uniform dispersion of the nanoparticles in the matrix with the structural integrity of CNTs, to improve the interfacial bonding, and mechanical properties of composites. Several processes are available for the uniform mixing of CNTs with aluminum powder, and each process has its advantages. This research aims to compare ball-milling with the solution-mixing process for uniform distribution of CNTs on the Al surface and analyze surface and structural deformation of both composites using field emission scanning electron microscopy (FESEM), high-resolution transmission electron microscopy (HRTEM), X-ray diffraction (XRD), particle size analyzer, Raman spectroscopy, and thermogravimetric analysis (TGA). Homogeneous reinforcement distribution in the metal matrix is required while maintaining the structural integrity of the CNTs to enhance mechanical and thermal properties.

2. EXPERIMENTAL PROCEDURE

2.1. Materials Used in the Study. Multiwall carbon nanotubes (MWCNTs) from Ad-Nano Technologies Pvt. Ltd. were used for the experiment. These CNTs had approximately 10−30 nm diameters and lengths ranging from 5 to 15 μm. 99% pure aluminum powder was received from Sigma-Aldrich Co. Ltd. The aluminum particles had a granular structure and varied in size between 5 and 80 μm. A combination of conventional ball-milling and a unique solution-mixing process was employed to effectively blend the CNTs with the aluminum powder to ensure a homogeneous mixture. Three distinct samples were synthesized for comparison, including aluminum powder without CNTs (Al), ball-milled aluminum with CNT nanocomposites (Al_{BM}), and aluminum with CNT nanocomposites produced using the solution-mixing process (Al_{SM}).

2.2. Ball-Milling Process. The method of ball-milling is adaptable and has a wide range of uses. It is a somewhat easy and affordable procedure that can be used to prepare a variety of materials. It is crucial to keep in mind, nevertheless, that ball-milling can also induce flaws into materials; thus, it is crucial to properly regulate the process variables in order to reduce these flaws. Carbon nanotubes (CNTs) may be dispersed in aluminum via a high-energy mechanical process called planetary ball-milling. The CNTs and aluminum powder are mixed in a spinning planetary mill that has several tiny vials or jars in it. The vials are subjected to intense impact pressures while the mill turns, which reduces the CNTs to smaller fragments and disperses them throughout the aluminum powder. Aluminum-CNT composites with excellent strength, stiffness, and electrical conductivity may be produced by using

https://doi.org/10.1021/acsomega.3c04531
ACS Omega 2023, 8, 33845−33856

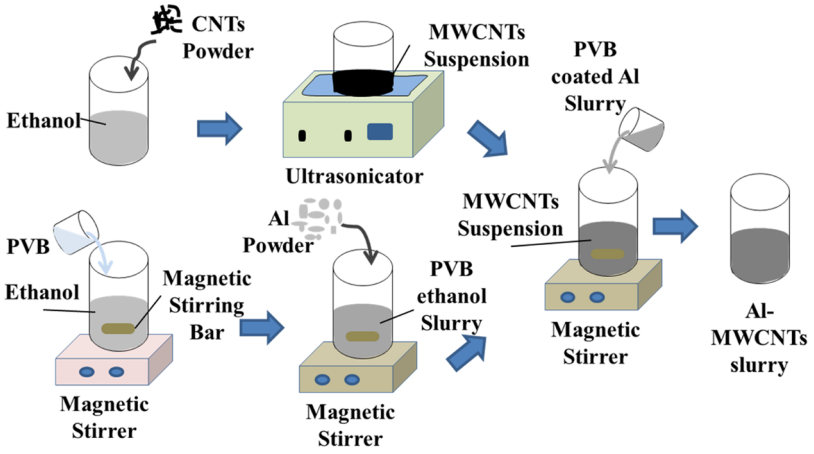

Figure 2. Schematic representation of processing steps used in the solution-mixing process for MWNT/Al composites.

this method. The procedure of planetary ball-milling is flexible and may be utilized to produce a range of aluminum-CNT composites with various characteristics. The kind of CNTs utilized, the quantity of CNTs used, the size of the CNTs, the type of aluminum powder used, and the milling process parameters will all affect the qualities of the composite. Some advantages of mixing CNTs with aluminum in a planetary ball mill are as follows: The CNTs may be dispersed throughout the aluminum powder by a high-energy procedure that can break them down into smaller bits. The CNTs are distributed more evenly as a result, which can increase the composite's strength, stiffness, and electrical/thermal conductivity. It moves along rather quickly. The milling procedure is feasible for industrial production since it may be finished in a couple of hours. It is an economical procedure. The planetary ball-mill's price is quite modest, as are the consumables (such CNTs, aluminum powder, and solvent). In general, planetary ball-milling is a flexible and economical method that may be utilized to produce a range of aluminum-CNT composites with various characteristics.

The process of combining the CNTs and Al powder involved using a planetary ball mill (Retsch 400), as illustrated in Figure 1 in the present study. Measures were taken to maintain the mixing jar and balls' cleanliness to prevent contamination of the samples. To clean the milling jar and ball, we put milling balls and cleaning solvent (dishwasher with some water) in a milling jar and carry out milling for half an hour to remove any unwanted particles that stick on the ball or jar surface. After milling, the jar and balls were washed and dried properly. Lastly, we use acetone to clean the ball and jar surface before the experiment. A mixture containing 0.5 wt % CNTs and 20 g Al powder was prepared in a stainless steel blending container. Stainless steel milling balls with a diameter of 5 mm were inserted at a weight ratio of 10:1. Furthermore, to avoid excessive cold-welding of the powder composites, during the ball-milling procedure, stearic acid was added to the powder mixes at a concentration of 1 wt %. Argon gas has been used to provide the inert milling condition. The ball mill ran at 200 rpm, and agitation was carried out for 6 h. The milling parameters were chosen from previous results[34,35] for effectively dispersing the CNTs with Al powder. After the mixture was mixed, samples were removed from the jars and sieved to separate the powder from steel balls. To assess the microstructure of the composite particles and the dispersion of CNTs inside the Al powder, the same experiment was performed two times to confirm the obtained result.

2.3. Solution-Mixing Process. The process of blending two or more compounds in a liquid solvent is known as solution-mixing. Material types include solids, liquids, and gases. The solubility of the components is used to determine the solvent. The components are combined to ensure that they are dispersed equally throughout the solvent. The technique of solution-mixing is adaptable and can be used to produce a range of goods. It is employed in the chemical, pharmaceutical, food, and beverage industries.

There are several approaches to solution-mixing. Utilizing a mechanical mixer is the most popular technique. Turbulence in the solution is produced by rotating impellers in mechanical mixers. The components are broken down and distributed uniformly throughout the solution owing to turbulence. The individual application, such as the solution-mixing method, determines the solution-mixing method to be used. Nanoparticles and other small materials can be blended by using high-pressure homogenization or ultrasonic mixing. Mechanical mixers can be used to combine larger materials such as powders. Less viscous solutions are easier to combine than more viscous ones. It is possible that mechanical mixers are ineffective in blending viscous fluids. For the combination of viscous fluids, ultrasonic mixing or high-pressure homogenization may be more efficient. The particular application determines the appropriate degree of mixing. For instance, a food product could just require mixing until the components are dispersed equally. To make certain that the chemicals are dispersed equally and that the result is free of impurities, a pharmaceutical product may need to be mixed to a considerably higher level. The technique of solution-mixing is adaptable and may be used to produce a range of goods. The particular application determines the solution-mixing technique that must be used.

In the solution-mixing process, first of all, CNTs (0.5 wt % Al) were added into ethanol (100 mL), and pristine CNTs bundles were separated into individual tubes using an ultrasonic bath for 4 h. Meanwhile, poly(vinyl butyral) (PVB) in equal weight of CNTs was separately added in 100 mL of ethanol. In as-produced PVB-ethanol solution, pure Al powder (50 g) was added and stirred using a magnetic stirrer for 3 h at 450 rpm. A thin PVB-coating was used to lower the surface tension and improve the Al particles' surface characteristics. 100 mL of PVB-coated Al slurry was then mixed with

https://doi.org/10.1021/acsomega.3c04531
ACS Omega 2023, 8, 33845−33856

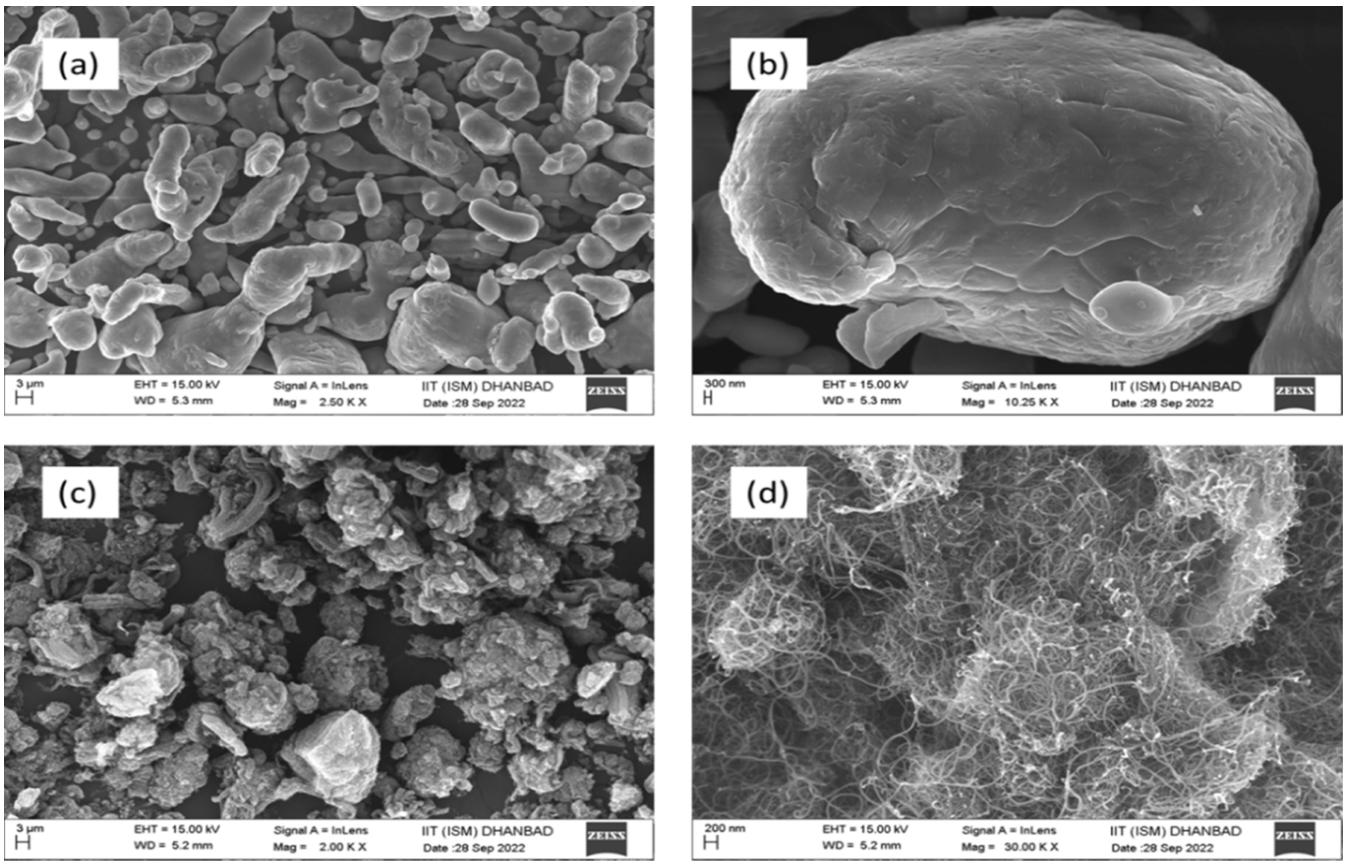

Figure 3. FESEM micrograph of (a) aluminum powders; (b) aluminum particle under higher magnification; (c) CNT clusters; and (d) CNT clusters under high magnification.

100 mL of MWNTs-ethanol solution. Stirring the mixture with a magnetic stirrer at 400 rpm for 4 h facilitated the uniform distribution of MWNTs in the aluminum matrix. Figure 2 displays a schematic illustration of the solution-mixing process. The homogenized composite slurry was dried in a vacuum filter, being exposed to a temperature of 100 °C for 24 h. The dried sample was agitated in a jar containing steel balls for 10 min, breaking down any lumps in the composite and forming uniform composite powders. These samples were characterized to confirm the CNT dispersion and morphology of the Al surface after mixing.

2.4. Fabrication of Composites. Composites are substances created from two or more distinct substances. When various components are mixed, a material is produced that has qualities that surpass those of the constituent parts. A metal powder and a reinforcing material can be combined to make composites by using PM. A fiber, ceramic, or another metal might be used as the reinforcing material. The metal powder is mixed with the reinforcing material in a precise ratio to produce a composite with the required characteristics. A variety of composites may be produced using the powder metallurgy method, which is a flexible procedure. Complex forms may be produced using this method, which is rather inexpensive.

The as-received Al, ball-milled, and solution-mixed composite powders were compacted under 600 MPa pressure in an H13 steel mold 20 mm in diameter. Prior to sintering, the powder composite was compacted with a universal testing machine (UTM). A thin layer of graphite spray was applied between the powder sample and the die wall to make it easy to remove the compressed sample after compression. By exerting pressure, the voids in a material are reduced during compaction. Rolling, tamping, and vibrations are a few techniques that may be used to accomplish this. In building, compaction is frequently utilized to increase the powder-carrying capacity, lessen settling, and enhance drainage.

Compaction may be divided into two categories: static and dynamic compaction. The method of continuously exerting pressure on a material over time is known as static compaction. Applying a rapid and powerful force to a material is the process of dynamic compaction. Here are the two primary compaction mechanisms: The process of moving and rearranging particles to bring them closer together is known as particle rearrangement. Numerous processes, such as rolling, tamping, and vibration, might cause this. Under pressure, particles undergo a process known as particle deformation. The particles may flatten, elongate, or even shatter as a result of this. The characteristics of the material being compacted and the amount of pressure applied determine the relative relevance of these two processes. In general, particle deformation is more significant for hard materials than particle rearrangement is for soft materials. The compacted pallets were sintered at 873 K for 2 h in a tube furnace with a continuous supply of argon gas (purity: 99.99%) until the furnace cooled to ambient temperature. Through this procedure, necks develop between the nearby powder particles. Atoms from the particles diffuse into the neck area, resulting in the formation of necks. The temperature, particle size, and surface energy of the particles all affect how quickly the neck grows. This is the method used to remove pores from sintered materials. The development of

https://doi.org/10.1021/acsomega.3c04531
ACS Omega 2023, 8, 33845−33856

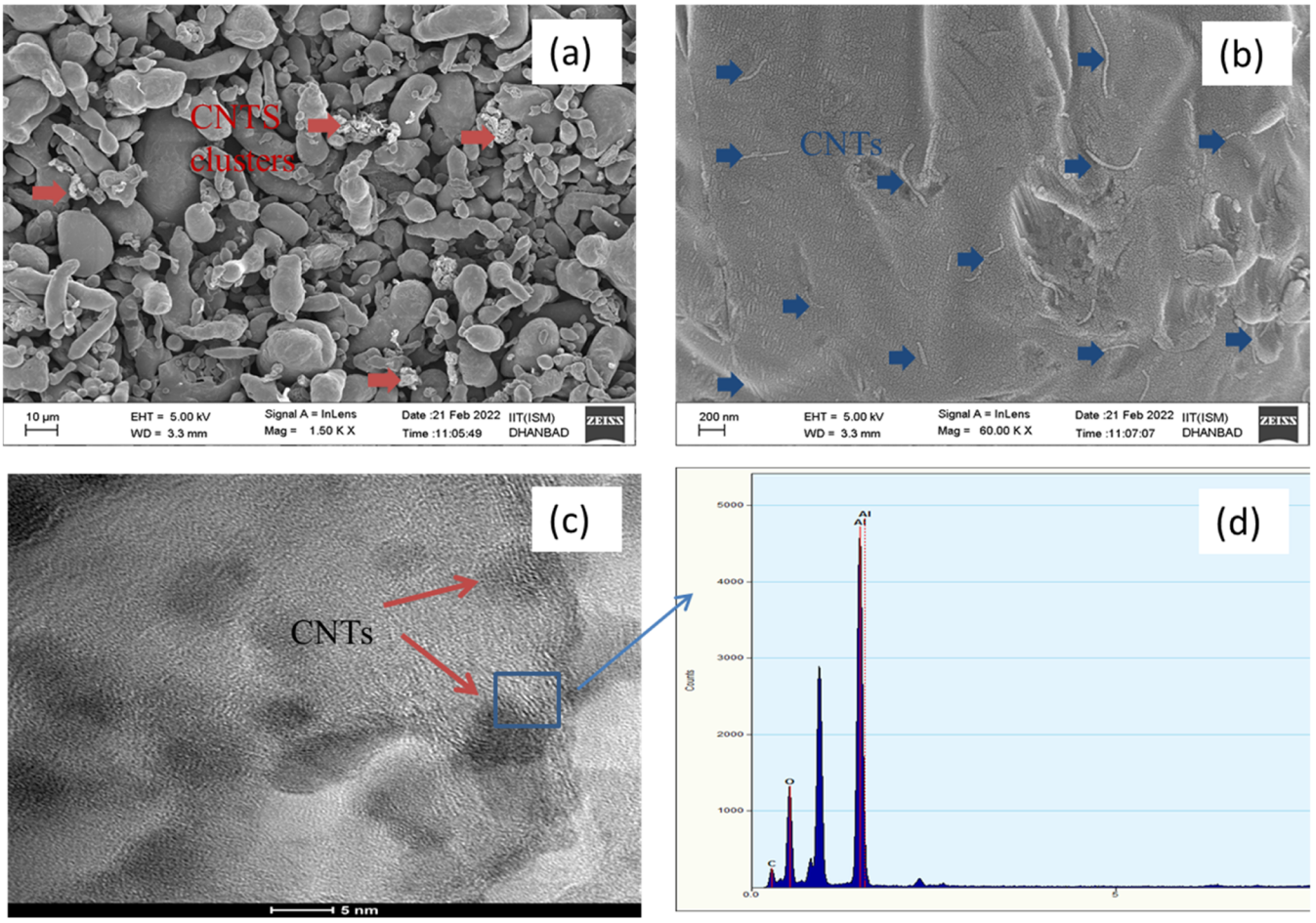

Figure 4. FESEM micrograph of ball-milled (a) Al composite; (b) Al composite under higher magnification; (c) TEM image of Al composite; and (d) EDS analysis of Al composite.

necks between neighboring particles eliminates pores. The pores are eventually eliminated when the necks develop and fuse together. Finally, these sintered bulk samples were gradually heated over 803 K in the furnace before being extruded into composite rods with an extrusion ratio of four.

2.5. Material Characterization. The characterization of CNT morphology and distribution on aluminum surfaces involved using field emission scanning electron microscopy (Zeiss Supra-55). A thin nanometer-scale layer of palladium (Pd) was applied as a coating on all samples to prevent powder sample surface charging during FESEM scanning. The dispersion and structure of CNTs were examined by using a high-resolution transmission electron microscope (HRTEM) (Thermo Scientific-Talos F200X G2). For determining the size distribution of the original aluminum powder, ball-milled samples, and solution-mixed powder composites, a laser diffraction particle size analyzer (PSA-1190) was utilized. The powder samples were dispersed in isopropyl alcohol and placed in an analytical glass tube for size analysis. To record the intensity pattern of the sample in the 20−80 range of 2θ, X-ray diffraction analysis (XRD) (from Rigaku Smartlab) was carried out. The Williamson−Hall equation was used to compute the crystal size and residual strain in accordance with various authors' methods.[36] Raman spectroscopy (LabRAM HR-UV-Open) was used to determine defects and impurities in the composite powder and the presence of CNTs in composites.

Tensile strength tests were used to evaluate the mechanical characteristics of the composite materials' mechanical characteristics. Microhardness measurements were conducted using a (Mitutoyo-HM220) Vickers microhardness system sourced from Japan, applying a loading weight of 200 g for a dwell time of 15 s. Each specimen underwent 10 measurements, and the average value was used to determine the hardness. A universal material testing device (Instron 8801, U.K.) was used to conduct tensile tests with a nominal strain rate of 1.010−4 s^{-1}. For the tensile testing, dog-bone-shaped specimens with gauge lengths of 20 mm and gauge widths of 4 mm were created. A crosshead speed of 0.5 mm/min was used for the experiments, which were carried out at room temperature with two samples per condition. A thermogravimetric analyzer (TGA) (NETZSCH Jupiter STA 449F3) was utilized to evaluate the thermal stability of the composite materials.

3. RESULT AND DISCUSSION

3.1. Microstructural Analysis of Composites Powder. The FESEM image in Figure 3 depicts the morphologies of raw Al and CNT powders. Al powder was irregular in shape, with a size ranging from 5 to 80 μm, as shown in Figure 3a,b. The pristine CNT clusters of larger size are observed in Figure 3c. Under high van der Wall force, CNTs clustered and formed particles with a size of about 50 μm. In Figure 3d, Nanotube entanglement and close packing due to their large surface area, aspect ratio (length-to-diameter ratio), and flexibility are

https://doi.org/10.1021/acsomega.3c04531
ACS Omega 2023, 8, 33845−33856

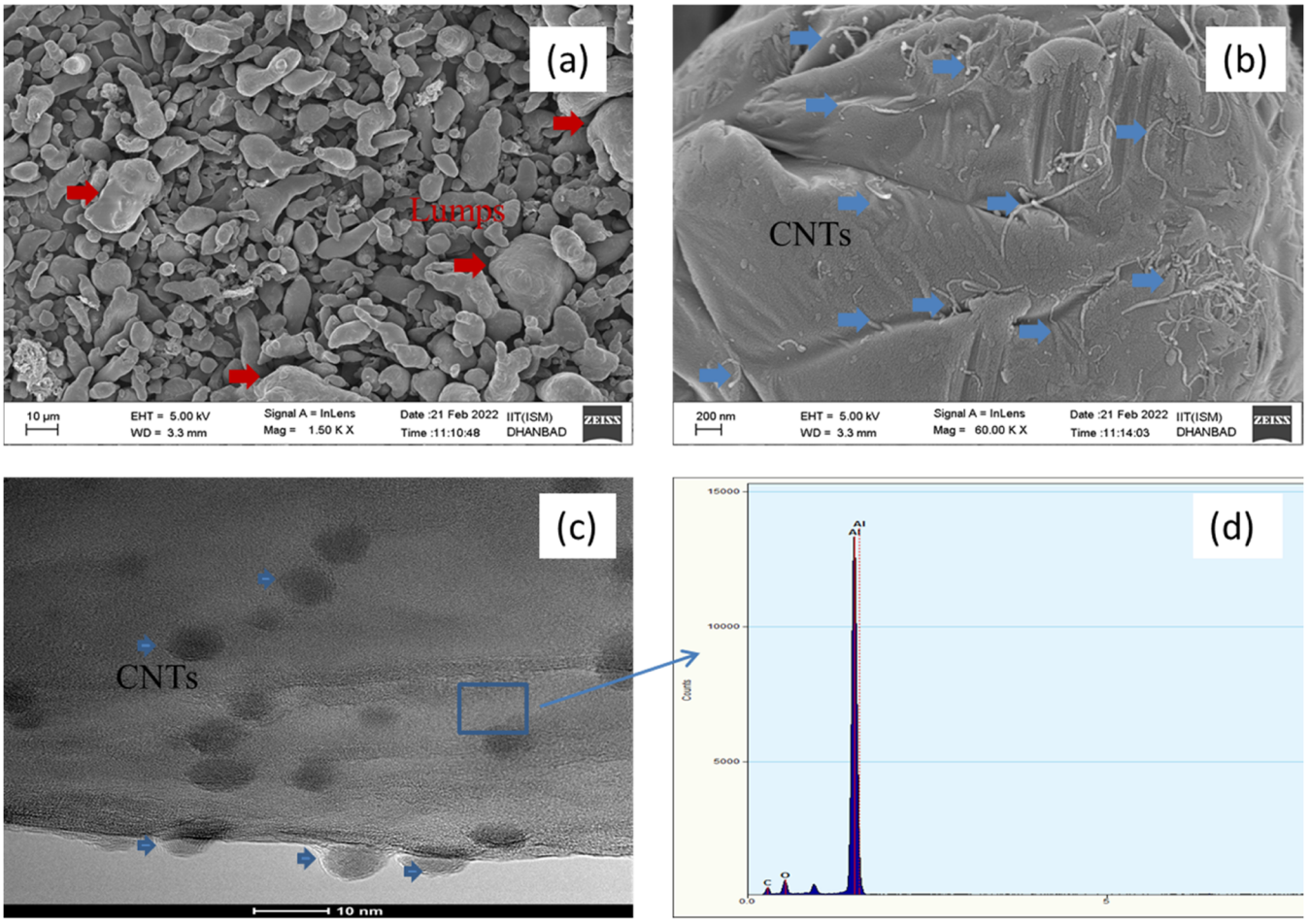

Figure 5. FESEM micrograph of solution-mixed (a) Al composite; (b) Al composite under higher magnification; (c) TEM image of Al composite; and (d) EDS analysis of Al composite.

identified. The high-resolution FESEM image revealed that the structure of pristine CNTs had an average diameter of 120 nm and a length of 3 μm. This study discovered a very high aspect ratio of CNTs, i.e., about 25.

When the ball-milled powder samples were investigated to observe the distribution of CNT particles with an Al matrix, in microscopic analysis, the author confirmed the clustering of CNTs in composite powder during milling, as shown in Figure 4a. This might be possible due to the large difference in Al and CNT particle size. Esawi et al.[32] also observed that larger-diameter CNTs had better dispersion within the Al matrix than smaller-diameter CNTs, which tended to agglomerate during milling. The larger interfacial contact surfaces of the smaller-diameter CNTs with the matrix materials reduced particle cold-welding during milling. A high-resolution field emission scanning electron microscope (FESEM) was used to analyze the morphology and CNT dispersion in the composite powder after milling, as shown in Figure 4b. Prolonged milling resulted in the shortening of CNTs and their embedding within the Al powder, facilitated by plastic deformation of the Al matrix caused by the impact of the milling ball. Figure 4c confirms the embedded CNTs in Al particles. CNT cross sections were clearly seen during the TEM analysis of ball-milled powder. To confirm the presence of Al and CNTs, EDS was performed, as shown in Figure 4d. The other peaks were present due to Cu Grit used for the TEM analysis.

Along with the dispersion of CNTs, the effect of the milling ball on Al and CNT particles is also observed. The collision impacts of the ball during the milling process start the microforging of aluminum particles and initiate changes in their shape, flattening and forming some flake-like shapes. The rough surface of flake particles gets smoother as the milling progresses.[37] In the ball-milling process, two intermittent processes are involved: cold working on powder, reducing the ductility of Al particles and ultimately reducing particles. The other is cold-welding of powder, responsible for increasing the particle size. Since Al is a very ductile material, the deformation of aluminum particles more often results in large particles. When CNTs were added, it reduced the ductility of composite powder and particle size. Esawi et al.[35] reported that the CNT-Al powder combination showed a flake-like morphology during the initial phases of ball-milling without the addition of any process control agent. However, the combination powders' morphology changed from a flake-like structure to a more granular shape as the ball-milling time rose. This transition is explained by the gradual development of a dynamic equilibrium between particle fracture and aggregation.

In the solution-mixing process, clusters of CNTs were absent. However, the fine composite powder gets agglomerated, forming lumps when the sample is dried after solution-mixing on the hot plate with continuous stirring, as shown in Figure 5a. It suggests that only magnetic stirring is insufficient to overcome wet agglomeration defects. To solve the problem

https://doi.org/10.1021/acsomega.3c04531
ACS Omega 2023, 8, 33845−33856

of composite powder cluster after solution-mixing, the dry composite powder, along with some steel ball bearings, was placed into a jar and shaken for 10 min, breaking the composite powder cluster and blending it uniformly. The shaking speed was very low, which does not show any impact of the steel ball on particle size and does not deform the surface of composite particles, which is favorable for the powder compaction, sintering process, and mechanical properties of the composites. The observed lumps in the composite powder were found to possess a soft and easily breakable nature when subjected to agitation with steel balls. The FESEM image presented in Figure 5b demonstrated the dispersion of individual CNTs throughout the surface of the aluminum powder in the Al-0.5 wt % CNT composite powder obtained through the solution-mixing process. These dispersed CNTs exhibited consistent size and length, resembling the characteristics of pure CNTs. This suggests that the aluminum and CNTs retained their original properties, including the size, shape, and morphology, even after mixing. Notably, the composite powder obtained through the solution-mixing procedure showed no signs of welded aluminum particles, which can be a significant issue when using high-energy dry ball-milling with aluminum powder. Further evidence of the presence of CNTs was provided by the TEM image in Figure 5c, which showed how they were distributed across the surface of the aluminum particles. The examination of energy-dispersive X-ray spectroscopy (EDS), as seen in Figure 5d, was done to offer more proof that CNTs are present on the aluminum surface.

Due to the addition of a dispersant, Al particles get coated with PVB, which reduces the surface tension of Al particles. CNTs easily dispersed on the Al particle surface in solution without any structural damage, i.e., significantly beneficial to achieve better properties of composites. During dispersion, when Al powder is added into the CNT dispersed solution, the mobility of CNTs in the matrix decreases due to the large particle size of the matrix. The large particles obstruct the free motion of CNTs and hinder their disintegration and uniform dispersion. Hence, researchers suggest using small aluminum particles with CNTs with relatively less resistance, and more dispersed composites can be achieved.

A phase transition during the mixing process was looked for using XRD analysis. The XRD spectra of pure aluminum and the composites (Al-0.5 wt % CNTs powder) produced through ball-milling and solution mixing are shown in Figure 6. As can be seen in the XRD pattern, pure Al showed strong characteristic peaks at 38, 44, 65, and 78° of 2θ.[38] The as-produced composite powder also shows an approximately similar peak to that of pure Al powder. These indicate no phase transformation during the mixing process. The XRD peaks of Al and their powder composites define the crystalline nature of the material.

X-ray diffraction (XRD) data may be used to calculate the crystallite size and lattice strain of a material by using the Williamson−Hall (WH) technique. The technique is based on the observation that an XRD peak's breadth is influenced by the size of the material's crystallites as well as the degree of lattice strain. For measuring the size and strain of the materials, the WH technique is an effective instrument. It may be used on a variety of different materials and is quite simple to apply. The technique does have significant drawbacks. For instance, the orientation of the crystallites is considered to be random. The WH technique may not produce reliable findings if the

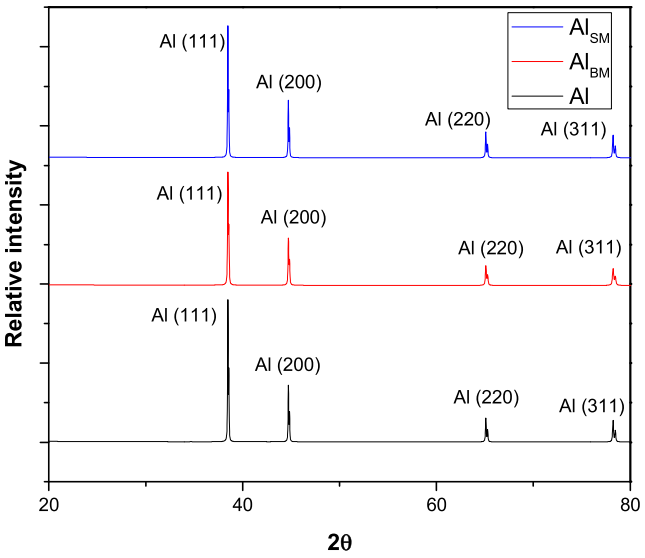

Figure 6. XRD analyses of as-received Al, Al_{BM}, and Al_{SM} composite powders.

crystallites are not randomly aligned. For material scientists and engineers, the Williamson−Hall approach is a useful tool. It may be used to learn more about the composition and characteristics of materials, which could help them perform better in practical applications. Using the Williamson−Hall equation (eq 1), the average crystalline size of pure Al and composite powder was determined[26]

$$\beta_{total} \cos\theta = 4\varepsilon \sin\theta + \frac{K\lambda}{L} \quad (1)$$

where β_{total} is the integral width of the XRD peak due to the crystalline size and microstrain, ε is the microstrain in grain, λ is the wavelength of XRD radiation (λ = 0.1540), and K is the Scherrer constant (K = 0.94). The above equation can be written in the form of $Y = mX + C$ and the graph plotted using the X-axis as $4\sin\theta$ and the Y axis as $\beta_{total}\cos\theta$. The slope of this curve will give us microstrain in grain, and the intercept will provide the crystalline size.

The calculated (using the intercept of W−H fitting) crystalline sizes of pure Al and as-produced Al_{BM} and Al_{SM} composite powders are 60.34, 55.69, and 60.81 nm, respectively. It suggests a small change in the grain size because the milling speed was slow (200 rpm), and the size of the ball was small. If the milling speed and size of the milling ball increased, it produced a finer crystalline structure in composite powder. The slope of W−H fitting indicates macrostrain in composites. In Figure 7, Al_{BM} shows more macrostrain than Al_{SM}. Achieving sufficiently high strength and stiffness in the bulk materials would be advantageous if the structure of the CNTs and the aluminum particle stayed mostly the same during ball-milling. It was noticed that no carbon peak was found in the composite powder; instead, it was present in it. The XRD signal is dependent on the crystal's volume; therefore, interference from various atomic layers must be constructive. The diffraction signal produced by surface layers and nanocrystals is usually much weaker than the XRD signal originating from the metal matrix. CNTs are not visible in the MMCs' XRD pattern; hence, Raman spectroscopy was used to detect them.

https://doi.org/10.1021/acsomega.3c04531
ACS Omega 2023, 8, 33845−33856

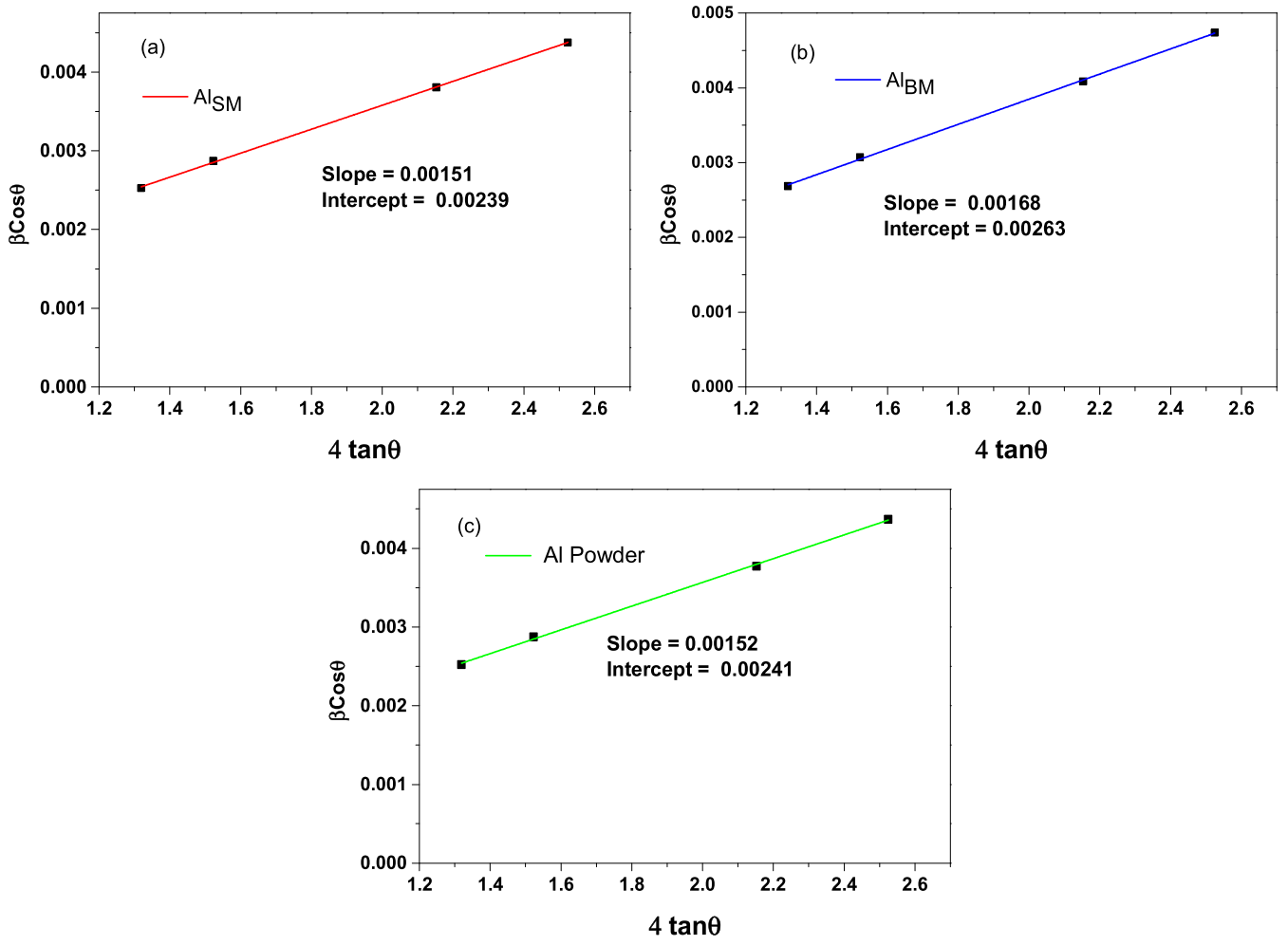

Figure 7. Williamson–Hall plot of (a) Al_{SM} composites, (b) Al_{BM} composites, and (c) pure Al powder.

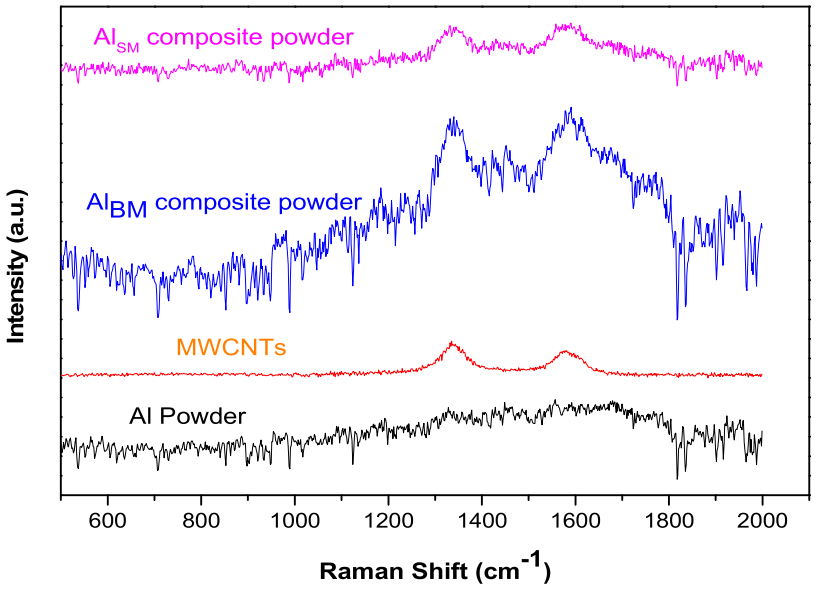

Figure 8. Raman spectra for Al, CNTs, and CNT-Al MMC powders after ball-milling and solution-mixing.

Raman spectroscopy is a nondestructive analytical technique that may be used to locate and quantify the individual components of a composite mixture. It operates by using a laser beam to excite the molecules in a substance and then observing the light that is reflected by the molecules. A mixture's various components may be distinguished from one another by using the distinctive Raman spectra they exhibit. For the investigation of composite mixtures, Raman spectros-

https://doi.org/10.1021/acsomega.3c04531
ACS Omega 2023, 8, 33845−33856

copy is a useful instrument for a variety of reasons. It is nondestructive, which implies that the sample is not harmed. Additionally, using it is quick and simple. Numerous types of materials, including metals, ceramics, and polymers, may be identified by using Raman spectroscopy. The concentrations of various ingredients in a combination may also be measured using this method.

In the present study, Raman spectroscopy was used to examine the distribution of CNTs in the composites following two distinct mixing methods and to validate their existence. In Figure 8, the Raman spectra of pure Al, Al-CNT composites, and CNTs as-received are contrasted. The D and G bands, which are located at 1341 and 1588 cm^{-1}, respectively, are clearly visible peaks in the Raman spectra of CNTs. The D band results from a double resonant Raman scattering mechanism, while the G band is related to the in-plane vibrations of carbon−carbon bonds.[23] Raman spectroscopy is widely used to assess the cleanliness of CNT samples and the existence of defects by comparing the intensities of the D and G Raman bands. The I_D/I_G ratio of the pure CNT sample in this investigation was found to be 1.32 ± 0.7, which is consistent with other studies. On the contrary, Raman spectra of the pure Al sample did not show any notable peaks, indicating that the bands seen in the Al-CNT composites in the 1000−2000 cm^{-1} range most likely came from CNTs ensconced in the Al matrix.

The Raman spectra of Al-CNT composites produced by the solution-mixing procedure resemble those of the CNTs that were initially received. The D and G bands' locations and configurations in the composites' Raman spectra closely mimic those seen in pure CNTs. However, there are observable variations in the Raman spectra of the ball-milled Al-CNT composites. The intensity of the D band is now stronger than that of the G band due to the extra flaws that the milling process generates. As a result, the I_D/I_G ratio increases when the D band becomes more prominent than the G band. The structural damage of CNTs from milling is shown by their greater I_D/I_G ratio.

In powder metallurgy industries, the uniform distribution of reinforcement and particle size are two important parameters responsible for the properties of composite materials and their final structure. The finer particles provide great strength and less porosity during the compaction and sintering. Table 1 shows the weight percentage of reinforcement, particle size (D_{50}), and the sample code used.

Table 1. Mean Particle Size of Pure Al and Composites

sample code	powder	reinforcement wt %	particle size (μm)
Al	pure Al	0	18.20
Al_{BM}	ball-milled	0.5	24.16
Al_{SM}	solution-mixing	0.5	19.17

The line graph depicted in Figure 9 illustrates the cumulative (PSD) particle size distribution of aluminum (Al), Al_{BM}, and Al_{SM} powders. The median particle size Z50, determined using the methodology of T. Peng,[39] corresponds to the particle size at which the cumulative distribution reaches 50%. Analysis of the graph reveals that the ball-milled composite (Al_{BM}) and solution-mixed composite (Al_{SM}) powders have median particle sizes Z50 of 24.6 and 19.17 μm, respectively, in comparison to the supplied pure Al powder with a particle size of 18.20 μm. Following the processing, the size of the

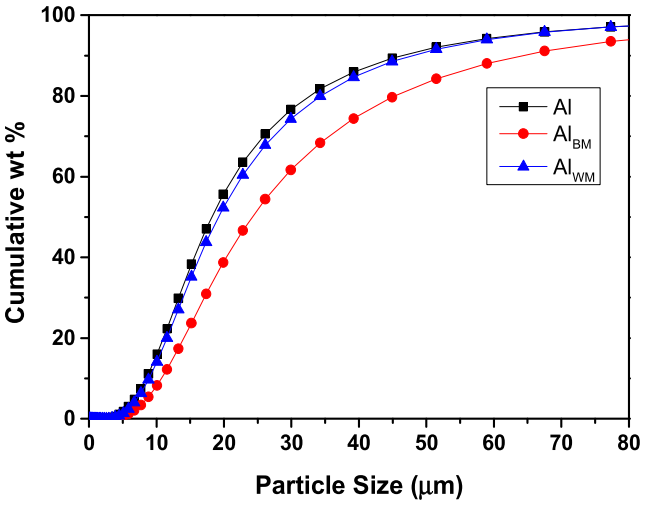

Figure 9. Particle size analysis of as-received Al and CNT-Al MMC powders after mixing.

composite particles exhibits a slight increase compared to the original Al powder. This phenomenon can be attributed to the relatively lower strength and stiffness of pure Al powder, resulting in plastic deformation when subjected to collisions with the milling ball. These findings affirm that the particle size of aluminum undergoes a shift toward larger sizes during ball-milling due to the deformable nature of Al powders. The observed deformation of the Al powder during milling leads to the formation of flake-shaped particles caused by the impact of the milling ball. Consequently, the dimensions of the particles increase along one direction while being reduced in another direction, ultimately contributing to an overall enlargement of the particle size. These flake-shaped powders have poor flowability, compatibility, and sintering ability that is not desired in the fabrication of composites by powder metallurgy. The structure of CNTs may also distort, which reduces the overall properties of composite materials. However, the solution-mixing process shows a similar particle size and shape as supplied Al has. The solution-mixing process produces CNTs distributed composite without any surface deformation. Hence, solution-mix composites have better surface properties as compared to ball-mill composites.

3.2. Mechanical Behaviors Influenced by Reinforcement. The effects of ball-milling and solution-mixing procedures on the microhardness and tensile characteristics of pure aluminum and CNT/aluminum composites are shown in Figures 10 and 11. The microhardness value of pure Al is determined to be 37 ± 0.8 Hv, whereas the ball-milled and solution-mixed CNTs/Al composites show 48.1 ± 1.1 and 49.8 ± 1.3 Hv, respectively. The tensile strength of pure Al is determined to be 157 MPa, and the elongation is measured at 20.0%, which aligns with the existing literature.[40] This consistency suggests that the designated metal-forming process yielded a dense microstructure. Compared to pure Al, the composites' hardness and tensile strength are improved by the addition of CNTs. The ball-milled composites demonstrated a 12% improvement in tensile strength and a 46% increase in hardness when compared to pure aluminum. The solution-mixed composites show a 50% improvement in hardness and a 14% increase in tensile strength when compared to pure aluminum. It is important to note that ball-milled composites have somewhat lower hardness and tensile strength than

https://doi.org/10.1021/acsomega.3c04531
ACS Omega 2023, 8, 33845−33856

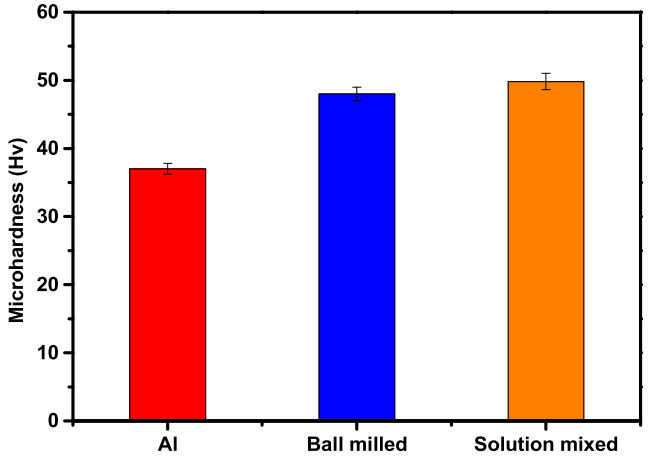

Figure 10. Effect of the Fabrication Process on the microhardness of CNT/Al composites.

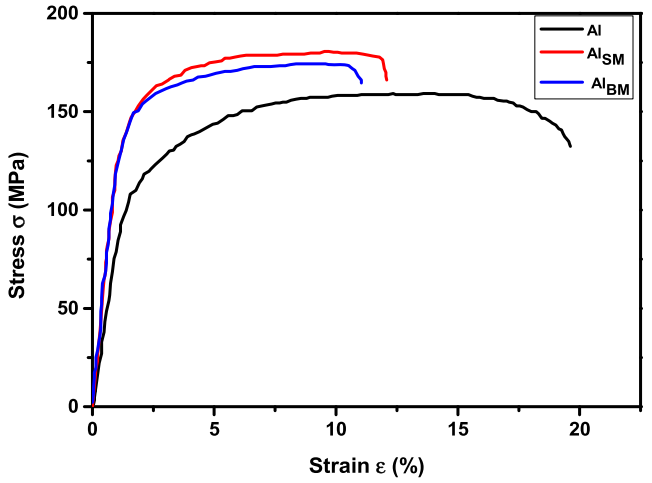

Figure 11. Effect of the fabrication process on the tensile properties of CNT/Al composites.

solution-mixed composites. This disparity can be attributed to the hardening of composite particles and structural damage incurred by the CNTs during the milling process.

Both the ball-milled and solution-mixed Al composites have less ductility than pure aluminum. According to earlier studies, the composites' tensile elongation reduces to 11 and 12%, respectively.[41] It is well-established that material strength and ductility have an inverse relationship, meaning that increased strength often comes at the expense of reduced ductility.[42] The homogeneous distribution of CNTs inside the Al matrix is projected to improve the mechanical properties of the CNT-reinforced composites by permitting efficient load transfer from the matrix to the reinforcement. Because of the firm interfacial bonding that occurs between the CNTs and the Al matrix during the tensile process, excellent CNT/Al composite load transfer is made feasible. Notably, the composites in this work have improved in terms of hardness and tensile strength, offering experimental support for the substantial role performed by CNTs in fortifying the finished composite. The solution-mixed composites show a uniform dispersion of CNTs without any structural damage and display strong interfacial interaction between the CNTs and the Al matrix, as seen in our earlier studies (Figures 4, 5, 8, and 9). This favorable microstructure ensures effective load transfer within the composite.

3.3. Thermal Stability. A material's capacity to tolerate heat without degradation is termed its thermal stability. Thermogravimetric analysis (TGA) is a method for calculating how much weight a substance loses when heated. This may be used to calculate the temperature at which a substance starts to burn or disintegrate. Because there is no oxygen in a nitrogen environment, nothing can oxidize or burn. This makes it possible to test the thermal stability of the material more precisely. The prepared sample's thermal stability was assessed using a thermogravimetric analyzer in a nitrogen atmosphere for a variety of reasons, including the following: to compare the thermal stability of various materials, to examine the effects of various processing conditions on a material's thermal stability, to quantify the amount of moisture or volatiles in a material, and because TGA is a flexible technique. It is a useful tool for figuring out the thermal stability of materials and forecasting how they will act in extreme heat.

The thermal stability of the prepared sample was evaluated using a thermo-gravimetric analyser in a nitrogen atmosphere. An alumina crucible containing approximately 6 to 8 grams of the sample was gradually heated from room temperature to 550 °C at a rate of 10 °C/min. The changes in mass during heating were recorded to determine the material's thermal stability, as shown in Figure 12. Notable distinctions were

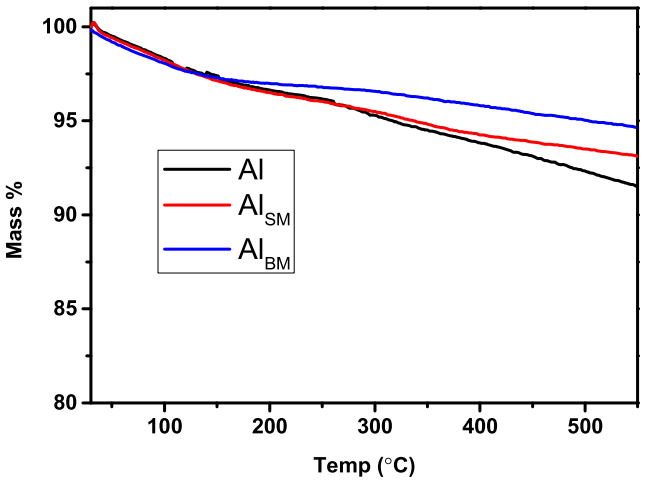

Figure 12. Weight loss versus temperature for the Al and Al-CNT composite samples.

observed between the composite samples (Al_{BM}, Al_{SM}) and the pure Al sample. The thermo-gravimetric curve of the pure Al sample exhibited significant variations with increasing temperature, displaying a continuous decrease throughout the entire temperature range. This reduction became more pronounced at higher temperatures

Conversely, the TGA curves of Al_{BM} and Al_{SM} samples appeared as nearly straight lines with minimal inclination at elevated temperatures. At 550 °C, the TG550/TG25 ratios were determined to be 92% for pure Al, 94% for Al_{BM}, and 95% for Al_{SM}. This dissimilarity in behavior between the Al and composite samples could be attributed to oxidation.[43] The linear TGA behavior and minimal weight loss indicated that the nanocomposite exhibited high thermal stability, further enhanced by the inclusion of CNTs as reinforcement in aluminum. Notably, at high temperatures, a slight downward

https://doi.org/10.1021/acsomega.3c04531
ACS Omega 2023, 8, 33845−33856

slope in the TGA curve of the solution-mixed composite suggested a change in the rate, likely associated with the rapid evaporation of organic molecules, resulting in weight loss.

4. CONCLUSIONS

The morphological evolution of CNT/Al composite powders and the mechanical properties of the thermal stability of the prepared sample were evaluated using a thermogravimetric analyzer in a nitrogen atmosphere. An alumina crucible containing approximately 6−8 g of sample was gradually heated from room temperature to 550 °C at a rate of 10 °C/min. The changes in mass during heating were recorded to determine the material's thermal stability, as shown in Figure 12. Notable distinctions were observed between the composite samples (Al_{BM}, Al_{SM}) and pure Al sample. The thermogravimetric curve of the pure Al sample exhibited significant variations with increasing temperature, displaying ball-milled and solution-mixed composites have been investigated. The following are the primary conclusions.

1. Solution-mixing is an effective process to disperse CNTs into an Al matrix without damage uniformly. XRD and Raman spectroscopy analyses observed structural deformation and generation of microstrain in the crystal due to milling. The I_D/I_G ratio of Raman spectra for solution-mixed composites was constant with CNTs, which is important for the improvement of composite properties.
2. After ball-milling, CNTs were discovered to be evenly distributed and imbedded in the Al matrix by TEM. However, in the solution-mixing process, CNTs uniformly dispersed on PVB-coated Al surface were observed.
3. In comparison to pure Al, the 0.5 wt % CNTs/Al composites show beneficial mechanical properties. The consolidated bulk composite, produced through the solution-mixing method, demonstrated a tensile strength of 176.0 MPa and an elongation of 121.4%. Due to the homogeneous distribution of CNTs throughout the composite and the finer grain structure of the Al matrix, these improved mechanical characteristics have been observed. These findings confirm the effectiveness of the solution-mixing process in fabricating CNT/Al composites with exceptional mechanical properties.
4. Thermogravimetric analysis revealed that adding MWCNTs stabilized the weight loss compared to pure aluminum, demonstrating that MWCNTs significantly improve the thermal stability of Al over the whole temperature range examined (25−550 °C).

AUTHOR INFORMATION

Corresponding Author

Shatrughan Soren − *Department of Fuel Minerals and Metallurgical Engineering, Indian institute of technology (Indian Schools of Mines), Dhanbad 826004, India;* orcid.org/0000-0002-5984-0042; Email: ssoren@iitism.ac.in

Authors

Navin Kumar − *Department of Fuel Minerals and Metallurgical Engineering, Indian institute of technology (Indian Schools of Mines), Dhanbad 826004, India*

Akhileshwar Nirala − *Department of Fuel Minerals and Metallurgical Engineering, Indian institute of technology (Indian Schools of Mines), Dhanbad 826004, India*

Naif Almakayeel − *Industrial Engineering Department, College of Engineering, King Khalid University, Abha 61421, Saudi Arabia*

T. M. Yunus Khan − *Department of Mechanical Engineering College of Engineering, King Khalid University, Abha 62529, Saudi Arabia;* orcid.org/0000-0002-9242-7591

Mohammad Amir Khan − *Department of Civil Engineering, Galgotias College of Engineering and Technology, Greater Noida 201310 Uttar Pradesh, India;* orcid.org/0009-0006-3612-8948

Complete contact information is available at: https://pubs.acs.org/10.1021/acsomega.3c04531

Notes

The authors declare no competing financial interest.

ACKNOWLEDGMENTS

The authors extend their appreciation to the Deanship of Scientific Research at King Khalid University for funding this work through research groups program under grant number (R.G.P 2/118/44).

REFERENCES

(1) Xie, S.; Li, W.; Pan, Z.; Chang, B.; Lianfeng, S. Mechanical and physical properties on carbon nanotube. *J. Phys. Chem. Solids* **2000**, *61*, 1153−1158.

(2) Ruoff, R. S.; Lorents, D. C. Mechanical and thermal properties of carbon nanotubes. *Carbon* **1995**, *33*, 925−930.

(3) Liu, C.; Naeem, S.; Lawler, S. P.; Woodfin, R. M.; Schlapfer, F.; Schmid, B.; et al. Hydrogen Storage in Single-Walled Carbon Nanotubes a t Room Temperature. *Science* **1999**, *286*, 1127−1129.

(4) Samuel Ratna Kumar, P. S.; Robinson Smart, D. S.; John Alexis, S. Corrosion behaviour of Aluminium Metal Matrix reinforced with Multi-wall Carbon Nanotube. *J. Asian Ceram Soc.* **2017**, *5*, 71−75.

(5) Zhang, S.; Han, X. Effect of different surface modified nanoparticles on viscosity of nanofluids. *Adv. Mech. Eng.* **2018**, *10*, No. 168781401876201.

(6) Bognár, G.; Vencl, A. Experimental Investigation of Viscosity of Glycerol Based Nanofluids Containing Carbon Nanotubes. *Tribol. Ind.* **2019**, *41*, 267−273.

(7) Menezes, B. R. C. d.; Rodrigues, K. F.; Fonseca, B. C. D. S.; Ribas, R. G.; Montanheiro, T. L. D. A.; Thim, G. P. Recent advances in the use of carbon nanotubes as smart biomaterials. *J. Mater. Chem. B* **2019**, *7*, 1343−1360.

(8) Wang, R.; Xie, L.; Hameed, S.; Wang, C.; Ying, Y. Mechanisms and applications of carbon nanotubes in terahertz devices: A review. *Carbon* **2018**, *132*, 42−58.

(9) Hvizdoš, P.; Vencl, A. Ceramic Matrix Composites With Carbon Nanophases: Development, Structure, Mechanical and Tribological Properties and Electrical Conductivity. In *Encyclopedia of Materials: Composites*; Elsevier, 2021; pp 116−133.

(10) Hvizdoš, P.; Duszová, A.; Puchý, V.; Tapasztó, O.; Kun, P.; Dusza, J.; et al. Wear Behavior of ZrO2-CNF and Si3N4-CNT Nanocomposites. *Key Eng. Mater.* **2011**, *465*, 495−498.

(11) Vencl, A.; Stojanović, B.; Gojković, R.; Klančnik, S.; Czifra, Á.; Jakimovska, K.; et al. Enhancing of ZA-27 alloy wear characteristics by addition of small amount of SiC nanoparticles and its optimization applying Taguchi method. *Tribol. Mater.* **2022**, *1*, 96−105.

(12) Stojanović, B.; Tomović, R.; Gajević, S.; Petrović, J.; Miladinović, S. Tribological behavior of aluminum composites using taguchi design and ANN. *Adv. Eng. Lett.* **2022**, *1*, 28−34.

(13) Stojanović, B.; Gajević, S.; Kostić, N.; Miladinović, S.; Vencl, A. Optimization of parameters that affect wear of A356/Al2O3

nanocomposites using RSM, ANN, GA and PSO methods. *Ind. Lubr. Tribol.* **2022**, *74*, 350−359.
(14) Fatile, B. O.; Adewuyi, B. O.; Owoyemi, H. T. Synthesis and characterization of ZA-27 alloy matrix composites reinforced with zinc oxide nanoparticles. *Eng. Sci. Technol.* **2017**, *20*, 1147−1154.
(15) Vencl, A.; Šljivić, V.; Pokusová, M.; Kandeva, M.; Sun, H.; Zadorozhnaya, E.; Bobić, I. Production, Microstructure and Tribological Properties of Zn-Al/Ti Metal-Metal Composites Reinforced with Alumina Nanoparticles. *Int. J. Metalcast.* **2021**, *15*, 1402−1411.
(16) Vencl, A.; Vučetić, F.; Bobić, B.; Pitel, J.; Bobić, I. Tribological characterisation in dry sliding conditions of compocasted hybrid A356/SiCp/Grp composites with graphite macroparticles. *Int. J. Adv. Manuf. Technol.* **2019**, *100*, 2135−2146.
(17) Yalçın, E. D.; Çanakçı, A.; Erdemir, F.; Çuvalcı, H.; Karabacak, A. H. Enhancement of Wear and Corrosion Resistance of ZA27/Nanographene Composites Produced by Powder Metallurgy. *Arab. J. Sci. Eng.* **2019**, *44*, 1437−1445.
(18) Fan, G.; Jiang, Y.; Tan, Z.; Guo, Q.; Xiong, D. bang.; Su, Y.; et al. Enhanced interfacial bonding and mechanical properties in CNT/Al composites fabricated by flake powder metallurgy. *Carbon* **2018**, *130*, 333−339.
(19) Jagannatham, M.; Chandran, P.; Sankaran, S.; Haridoss, P.; Nayan, N.; Bakshi, S. R. Tensile properties of carbon nanotubes reinforced aluminum matrix composites: A review. *Carbon* **2020**, *160*, 14−44.
(20) Park, J. G.; Keum, D. H.; Lee, Y. H. Strengthening mechanisms in carbon nanotube-reinforced aluminum composites. *Carbon* **2015**, *95*, 690−698.
(21) Srinivasan, V.; Kunjiappan, S.; Palanisamy, P. A brief review of carbon nanotube reinforced metal matrix composites for aerospace and defense applications. *Int. Nano Lett.* **2021**, *11*, 321.
(22) Udupa, G.; Shrikantha Rao, S.; Gangadharan, K. V. In *Future Applications of Carbon Nanotube Reinforced Functionally Graded Composite Materials*, IEEE-International Conference On Advances In Engineering, Science And Management (ICAESM -2012), 2012; pp 399−404.
(23) Suzuki, S.; Hibino, H. Characterization of doped single-wall carbon nanotubes by Raman spectroscopy. *Carbon* **2011**, *49*, 2264−2272.
(24) George, R.; Kashyap, K. T.; Rahul, R.; Yamdagni, S. Strengthening in carbon nanotube/aluminium (CNT/Al) composites. *Scr. Mater.* **2005**, *53*, 1159−1163.
(25) Azarniya, A.; Safavi, M.; Sovizi, S.; et al. Metallurgical Challenges in Carbon Nanotube-Reinforced Metal Matrix Nanocomposites. *Metals* **2017**, No. 384, DOI: 10.3390/met7100384.
(26) Kumar Tiwari, S.; Singh, H.; Midathada, A.; Sharma, S.; Ravella, U. K. Study of Fabrication Processes and Properties of Al-CNT Composites Reinforced by Carbon Nano tubes-A Review. *Mater. Today Proc.* **2018**, *5*, 28262−28270.
(27) Bakshi, S. R.; Agarwal, A. An analysis of the factors affecting strengthening in carbon nanotube reinforced aluminum composites. *Carbon* **2011**, *49*, 533−544.
(28) Deng, C. F.; Wang, D. Z.; Zhang, X. X.; Li, A. B. Processing and properties of carbon nanotubes reinforced aluminum composites. *Mater. Sci. Eng., A* **2007**, *444*, 138−145.
(29) Pérez-Bustamante, R.; Estrada-Guel, I.; Antúnez-Flores, W.; Miki-Yoshida, M.; Ferreira, P. J.; Martínez-Sánchez, R. Novel Al-matrix nanocomposites reinforced with multi-walled carbon nanotubes. *J. Alloys Compd.* **2008**, *450*, 323−326.
(30) Peng, T.; Chang, I. Mechanical alloying of multi-walled carbon nanotubes reinforced aluminum composite powder. *Powder Technol.* **2014**, *266*, 7−15.
(31) Choi, H. J.; Shin, J. H.; Bae, D. H. The effect of milling conditions on microstructures and mechanical properties of Al/MWCNT composites. *Composites, Part A* **2012**, *43*, 1061−1072.
(32) Esawi, A. M. K.; Morsi, K.; Sayed, A.; Taher, M.; Lanka, S. The influence of carbon nanotube (CNT) morphology and diameter on the processing and properties of CNT-reinforced aluminium composites. *Composites, Part A* **2011**, *42*, 234−243.
(33) Liu, Z. Y.; Zhao, K.; Xiao, B. L.; Wang, W. G.; Ma, Z. Y. Fabrication of CNT/Al composites with low damage to CNTs by a novel solution-assisted wet mixing combined with powder metallurgy processing. *Mater. Des* **2016**, *97*, 424−430.
(34) Pérez-Bustamante, R.; Gómez-Esparza, C. D.; Estrada-Guel, I.; Miki-Yoshida, M.; Licea-Jiménez, L.; Pérez-García, S. A.; Martínez-Sánchez, R. Microstructural and mechanical characterization of Al-MWCNT composites produced by mechanical milling. *Mater. Sci. Eng., A* **2009**, *502*, 159−163.
(35) Esawi, A.; Morsi, K. Dispersion of carbon nanotubes (CNTs) in aluminum powder. *Composites, Part A* **2007**, *38*, 646−650.
(36) Mote, V.; Purushotham, Y.; Dole, B. Williamson-Hall analysis in estimation of lattice strain in nanometer-sized ZnO particles. *J. Theor Appl. Phys.* **2012**, *6*, No. 6.
(37) Wang, L.; Choi, H.; Myoung, J. M.; Lee, W. Mechanical alloying of multi-walled carbon nanotubes and aluminium powders for the preparation of carbon/metal composites. *Carbon* **2009**, *47*, 3427−3433.
(38) Alanka, S.; Ratnam, C.; Prasad, B. S. An effective approach to synthesize carbon nanotube-reinforced Al matrix composite precursor. *Sci. Eng. Compos. Mater.* **2018**, *25*, 983−991.
(39) Peng, T.; Chang, I. Uniformly dispersion of carbon nanotube in aluminum powders by wet shake-mixing approach. *Powder Technol.* **2015**, *284*, 32−39.
(40) Chen, B.; Li, S.; Imai, H.; Jia, L.; Umeda, J.; Takahashi, M.; Kondoh, K. An approach for homogeneous carbon nanotube dispersion in Al matrix composites. *Mater. Des.* **2015**, *72*, 1−8.
(41) Jiang, L.; Li, Z.; Fan, G.; Cao, L.; Zhang, D. The use of flake powder metallurgy to produce carbon nanotube (CNT)/aluminum composites with a homogenous CNT distribution. *Carbon* **2012**, *50*, 1993−1998.
(42) He, C.; Zhao, N.; Shi, C.; Du, X.; Li, J.; Li, H.; Cui, Q. An approach to obtaining homogeneously dispersed carbon nanotubes in Al powders for preparing reinforced Al-matrix composites. *Adv. Mater.* **2007**, *19*, 1128−1132.
(43) Saadallah, S.; Cablé, A.; Hamamda, S.; Chetehouna, K.; Sahli, M.; Boubertakh, A.; et al. Structural and thermal characterization of multiwall carbon nanotubes (MWCNTs)/aluminum (Al) nanocomposites. *Composites, Part B* **2018**, *151*, 232−236.

https://doi.org/10.1021/acsomega.3c04531
ACS Omega 2023, 8, 33845−33856